Isomorphic Cd(II)/Zn(II)-MOFs as Bifunctional Chemosensors for Anion ($Cr_2O_7^{2-}$) and Cation (Fe^{3+}) detection in Aqueous Solution

Kai Chen[1,*], Ran Li,[1] Yu-Ying Peng,[1] Zhu-Qian Cai,[1] Zi-Yi Hua[1], Xiu-Du Zhang,[2] Carl Redshaw,[3] Yue Zhao[2,*]

[1] Collaborative Innovation Center of Atmospheric Environment and Equipment Technology, Jiangsu Key Laboratory of Atmospheric Environment Monitoring and Pollution Control, School of Environmental Science and Engineering, Nanjing University of Information Science & Technology, Nanjing 210044, P. R. China.
[2] Coordination Chemistry Institute, State Key Laboratory of Coordination Chemistry, School of Chemistry and Chemical Engineering, Nanjing National Laboratory of Microstructures, Collaborative Innovation Center of Advanced Microstructures, Nanjing University, Nanjing 210023, China.
[3] Department of Chemistry & Biochemistry, University of Hull, Hull HU6 7RX, UK.

Email: kaichen85@nuist.edu.cn or catQchen@163.com (K. Chen); zhaoyue@nju.edu.cn (Y. Zhao)

Abstract: Two isomorphic 3D MOFs [Cd(2-bpeb)(sdba)] (**1**) and [Zn(2-bpeb)(sdba)] derived from the π-conjugated pro-ligand 2-(4-((E)-2-(pyridine-2-yl)vinyl)styryl)pyridine (2-bpeb) and 4,4'-sulfonyldibenzoate (H_2sdba) were synthesized and characterized. Complexes **1** and **2** exhibit striking fluorescence properties and can function as chemical sensors via rapid luminescence quenching in the presence of $Fe^{3+}$and $Cr_2O_7^{2-}$ in aqueous media with high sensitivity and selectivity.

Keywords: Coordination polymers, Fluorescent sensors, Highly oxidizing anions, d^{10} metal ions.

Introduction

Due to the increasing levels of various pollutants associated with global industries, there is increased risk to human health, and this has attracted the attention of the general public, and there is now a demand for better pollution control. Among the pollutants, the management and detection of heavy metal ions and oxo-anions is of special concern because of their extensive use and high toxicity [1-2]. A widely used metallic material in industrial processes and an essential trace element of the human body is iron. However, it cannot be metabolized normally and this can lead to poisoning when iron is ingested or excessively absorbed by the body. Previous studies

have demonstrated that excessive Fe(III) can cause mental issues, lead to a lack of physical strength, and is responsible for a series of diseases[3]. On the other hand, as a well-known strong oxidant, dichromate $Cr_2O_7^{2-}$ is widely used in various industrial processes such as those that involve electroplating, paint, leather tanning and pesticides [4]. However, once it is allowed to seep into the environment, it poses a huge threat to living organisms, especially human health. Upon entering the human body, $Cr_2O_7^{2-}$ can damage internal organs such as the liver and kidney as well as DNA, and can induce genetic mutations and various cancers. A number of materials/methods have been applied to the detection of Fe^{3+} and $Cr_2O_7^{2-}$, however, they are not readily used in an aqueous environment and these traditional methods often suffer from being complicated and time-consuming to use, as well as possessing low sensitivity, low selectivity, and high associated costs.

As a relatively new type of porous crystalline material, metal-organic frameworks (MOFs) have attracted considerable attention over the past few years [5-11]. MOFs and related materials have shown excellent performance in gas storage [6] and separation [7], sensing [8], catalysis [9], photoelectricity [10] and energy storage [11]. Luminous MOFs have received attention because of their potential applications in sensory applications. Compared with other chemical sensors, those based on luminescent MOF materials offer more advantages due to their favorable sensitivity and selectivity, fast response time, operability and recyclability [12-14]. These attributes have led to their application in the sensing and identification of various analytes, including a variety of anions, cations, gases, small molecules, and explosives. Both Cd(II) and Zn(II) metal ions have previously been exploited in the assembly process of luminescent MOFs[15-20].

Herein, the π-conjugated pro-ligand 2-(4-((E)-2-(pyridine-2-yl)vinyl)styryl)pyridine (2-bpeb) and 4,4'-sulfonyldibenzoate (H_2sdba) were combined with d^{10} metal ions in order to design luminescent MOFs under solvothermal conditions, namely [Cd(2-bpeb)(sdba)] (**1**) and [Zn(2-bpeb)(sdba)] (**2**). The structural analyses indicate that complexes **1** and **2** are isomorphic and have similar framework structures. The sensing properties toward cations and anions have been further explored. The fluorescent investigations suggest that **1** and **2** can selectively sense $Cr_2O_7^{2-}$ and Fe^{3+} in aqueous systems with both high selectivity and sensitivity.

Experimental Section

Materials and General Methods.

All reagents and solvents were commercially purchased and were used as received without further purification. Pro-ligand 2-bpeb was synthesized according to the previous literature method [20]. Elemental analyses were performed on a PerkinElmer 240C Elemental Analyzer at the analysis center of Nanjing University. FT-IR spectra were recorded in the range of 400-4000 cm^{-1} on a Bruker Vector 22 FT-IR spectrophotometer using KBr pellets. Thermogravimetric analyses (TGA) were conducted on a Mettler-Toledo (TGA/DSC1) thermal analyzer under nitrogen with a heating rate of 10 °C min^{-1}. Powder X-ray diffraction (PXRD) data for all samples were collected at room temperature on bulk samples with Cu-Kα radiation (1.54059 Å) on a Bruker D8 Advance X-ray diffractometer, in which the X-ray tube was operated at 40 kV and 40 mA. The fluorescence spectra were recorded on a PerkinElmer LS-55 fluorescence spectrophotometer. UV-vis measurements were carried out at room temperature on a Shimadzu UV3600 spectrophotometer. Quantum yields and fluorescence lifetime measurements were performed on a HORIBA Jobin Yvon Fluoromax-4 spectrometer.

Preparation of [Cd(2-bpeb)(sdba)] (1)

A mixture of 2-bpeb (14.2 mg, 0.05 mmol), H_2sdba (15.3 mg, 0.05 mmol), $Cd(NO_3)_2 \cdot 4H_2O$ (11.8 mg, 0.05 mmol), *N*,*N*-dimethylformamide (DMF, 3 mL), H_2O (1 mL) and dimethyl sulfoxide (0.5 mL) were placed in a 10 mL glass bottle. The bottle was sealed and kept at 90 ℃ for 72 h. After being cooled to room temperature, yellow block crystals of **1** were obtained in 45% yield. Anal. Calcd for $C_{34}H_{24}N_2O_6SCd$: C58.25, H 24.19, N 3.99 %. Found: C 58.22, H 24.23, N 3.96%. IR (KBr pellet, cm^{-1}): 3447 (m), 2360 (w), 1682 (m), 1631 (s), 1601 (s), 1554(s), 1476 (m), 1439 (s), 1399 (w), 1381 (w), 1306 (w), 1291 (w), 1221(w), 1154 (s), 1126 (m), 1102 (m), 1068 (m), 1009 (m), 955 (w), 852 (w), 824 (m), 767 (s), 748 (m), 726 (w), 696 (w), 633 (m), 621 (w), 581 (w), 550 (m), 470 (m), 414 cm^{-1}(w).

Preparation of [Zn(2-bpeb)(sdba)] (2)

Complex **2** was prepared by the same procedure used for the preparation of **1** except that $Cd(NO_3)_2 \cdot 4H_2O$ were replaced by $Zn(NO_3)_2 \cdot 6H_2O$ (14.9 mg, 0.05 mmol). After being cooled to room temperature, yellow block crystals of **2** were obtained in 39% yield. Anal. Calcd for $C_{34}H_{24}N_2O_6SZn$: C 62.43, H 3.69, N 4.28 %. Found: C 62.41, H 3.72, N 4.21 %. IR (KBr pellet, cm^{-1}): 3445 (m), 3063 (w), 1682 (m), 1620 (s), 1564

(s), 1514(s), 1479 (m), 1441 (s), 1396 (w), 1359 (w), 1306 (w), 1290 (w), 1151(w), 1123 (s), 1102 (m), 1064 (m), 1022 (s), 1008 (m), 967 (w), 863 (w), 845 (m), 825 (m), 772 (s), 749 (m), 725 (w), 696 (w), 635 (m), 620 (w), 581 (w), 551 (m), 472 (m), 422 cm^{-1}(w).

X-Ray crystallography

The crystallographic data collection for **1** was carried out on a Bruker Smart Apex II CCD area-detector diffractometer with graphite-monochromated Mo-Kα radiation (λ = 0.71073 Å) at 293(2) K using the ω-scan technique, while data for **2** was collected on a Bruker D8 Venture Photon II diffractometer with graphite-monochromated Ga-Kα radiation (λ = 1.34139 Å). The diffraction data were integrated by using the *SAINT* program,[21] which was also used for the intensity corrections for the Lorentz and polarization effects. Semi-empirical absorption corrections were applied using the *SADABS* program.[22] The structures were solved by direct methods and all the non-hydrogen atoms were refined anisotropically on F^2 by the full-matrix least-squares technique using the SHELXL-97 crystallographic software package.[23] All non-hydrogen atoms were refined anisotropically. Hydrogen atoms of the water molecules were located from the difference Fourier maps and refined with restraint of the O-H and H···H distance (0.96 Å and 1.52 Å, respectively). Other hydrogen atoms were introduced at the calculated positions. The details of the crystal parameters, data collection and refinements for the complexes are summarized in **Table 1**, and selected bond lengths and angles with their estimated standard deviations are listed in **Table S1**. CCDC NO. 2015015 (**1**), and 2015016 (**2**).

Table 1. Crystal Data and Structure Refinements for **1 - 2**.

Complex	**1**	**2**
Formula	$C_{34}H_{24}N_2O_6SCd$	$C_{34}H_{24}N_2O_6SZn$
Formula weight	701.01	653.98
T (K)	193(2)	193(2)
Crystal system	Orthorhombic	Orthorhombic
Space group	*P*cca	*P*cca
a (Å)	24.855(5)	24.2175(19)
b (Å)	6.442(2)	6.5093(5)
c (Å)	21.169(4)	21.0076(15)
β (º)	90	90
V (Å^3)	3389.3(14)	3311.6(4)
Z	4	4
D_{calc} (g cm^{-3})	1.374	1.312
μ (mm^{-1})	0.750	0.890
F(000)	1416	1344
R_{int}	0.0607	0.0672
Reflections collected	3921	3044

Unique reflections	3135	2406
Goodness-of-fit on F^2	1.136	1.009
R_1,	0.0525	0.0398
wR_2 [I > 2σ(*I*)][a, b]	0.1105	0.1048
R_1,	0.0695	0.0547
wR_2 [all data]	0.1165	0.1143

[a] $R_1 = \Sigma||F_o| - |F_c||/\Sigma|F_o|$. [b] $wR_2 = [\Sigma w(|F_o|^2 - |F_c|^2)|/\Sigma|w(F_o)^2|^{1/2}$, where w = m= $1/[\sigma^2(F_o^2) + (aP)^2 + bP]$. P = $(F_o^2 + 2F_c^2)/3$

Results and Discussion

Crystal Structure Description

Single crystal X-ray diffraction (SC-XRD) analysis revealed that the complexes [Cd(2-bpeb)(sdba)] **1** and [Zn(2-bpeb)(sdba)] **2** crystallize in the orthorhombic crystal system with the same space group *P*cca. Given this, only the molecular structure of complex **1** is discussed herein. The asymmetric unit of **1** contains one Cd(II) ion, one 2-bpeb and one $sdba^{2-}$. As shown in **Fig. 1a**, each Cd(II) atom is located in a distorted regular octahedron coordination geometry surrounded by two nitrogen atoms (N1, N1#1) from two different 2-bpeb ligands and four oxygen atoms (O1, O2, O1#1, O2#2) provided by two distinct carboxylates from two $sdba^{2-}$ ligands. The Cd-N bond length is 2.250(3) Å and Cd-O distances are 2.250(3) and 2.574(3) Å. Each $sdba^{2-}$ ligand in **1** connects two Cd(II) atoms using its two carboxylate groups each via the $\eta^1:\eta^1$ monodentate mode. Ignoring the connection with $sdba^{2-}$, the 2-bpeb ligands produce one pair of 1D helix chains by linking Cd(II) atoms (**Fig. 1b**). A two-dimensional network (**Fig. 1d**) is formed by 1D 2-bpeb-Cd(II) helix chains through the bridging $sdba^{2-}$ ligand (**Fig. 1c**). The adjacent 2D layers are further constructed by non-covalent interactions (**Fig. 1e**), thereby resulting in the final three-dimensional framework of **1** possessing 1D channels (**Fig. 1f**).

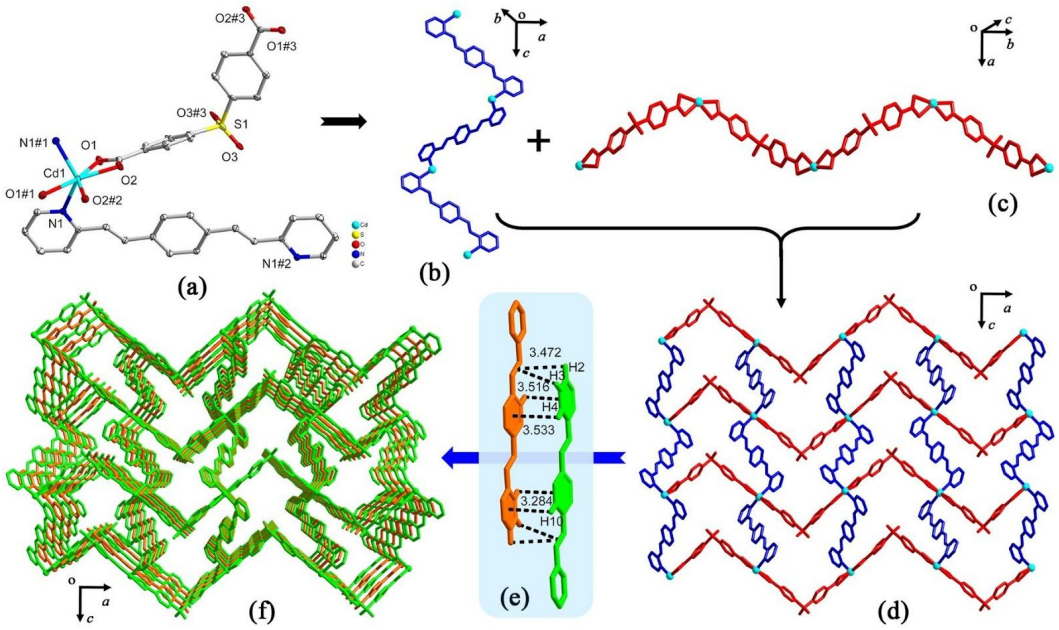

Fig. 1. (a) Coordination environment of Cd(II) in **1** with the ellipsoids drawn at the 30% probability level. The hydrogen atoms are omitted for clarity. (b) 1D 2-bpeb helix chain in **l**. (c) 1D "zigzag" chain in **l**. (d) 2D network (e) the detail non-convent interaction between the adjacent 2-bpep ligands from two different neighbouring layers. (f) 3D MOF of **1**.

Powder X-Ray Diffraction (PXRD) and Stability Studies

PXRD measurements were employed to confirm the bulk phase purity of the synthesized coordination polymers **1** and **2**. As shown in **Fig. 2**, the results of the PXRD measurements revealed that the peak positions of the obtained crystalline samples of **1** and **2** matched well with the simulated patterns obtained from the single-crystal diffraction data, confirming the phase purity of the synthesized samples.

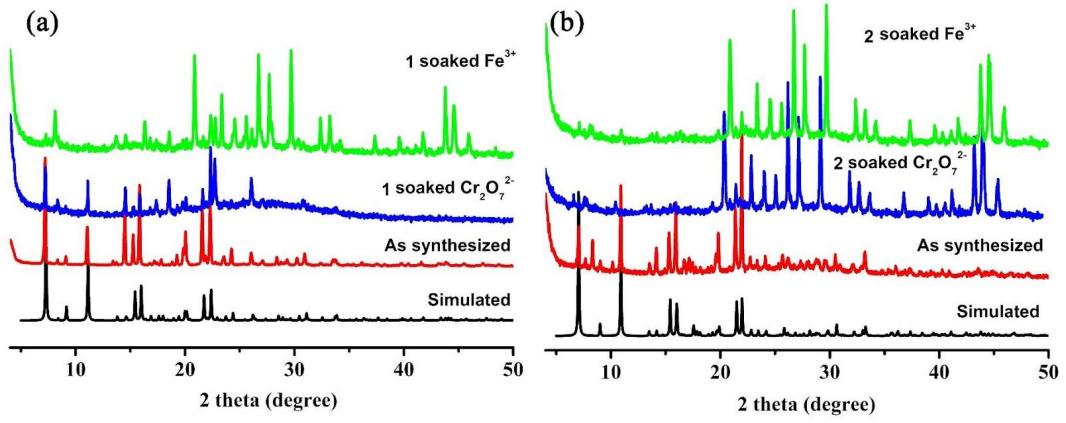

Fig. 2. PXRD patterns for **1**-**2** under ambient conditions: simulated (black) and as-synthesized (red), **1** and **2** before and after immersed in Fe^{3+} and $Cr_2O_7^{2-}$ water solution: (a) **1** and (b) **2**.

The thermal stability of **1** and **2** were examined by thermogravimetric analysis (TGA) and the results are depicted in **Fig. 3**. Complexes **1** and **2** show no obvious weight loss before the decomposition of the frameworks and are stable up to about

370 ℃ and 375 ℃, respectively.

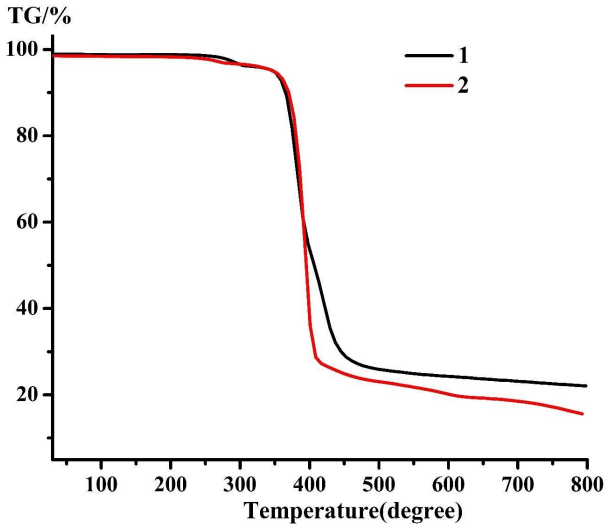

Fig. 3. TG curves of **1** and **2.**

Fluorescence properties

Metal complexes consisting of d^{10} metal atoms have been widely investigated as potential fluorescent materials.[24] Therefore, the fluorescence properties of complexes **1** and **2**, as well as the corresponding free 2-bpeb and H_2sdba, were investigated in the solid state at room temperature. As depicted in **Fig. 4**, the ligands 2-bpeb and H_2sdba exhibit an emission band at 490 nm and 320 nm upon excitation at 355 nm and 280 nm, respectively, while the emission bands of compounds **1** and **2** are observed at 498 nm and 505 nm under excitation at 381 nm and 384 nm, respectively. By comparing the emission bands of **1** and **2** with those of the original ligands, it can be assumed that the fluorescence emission of **1** and **2** is attributed to the ligand 2-bpeb. In addition, given that metal ions with d^{10} configurations are difficult to oxidize or reduce, the red shift of the emission maximum between the complex and the ligand can be ascribed to the coordination with the Cd(II)/Zn(II) metal centres.[25, 26]

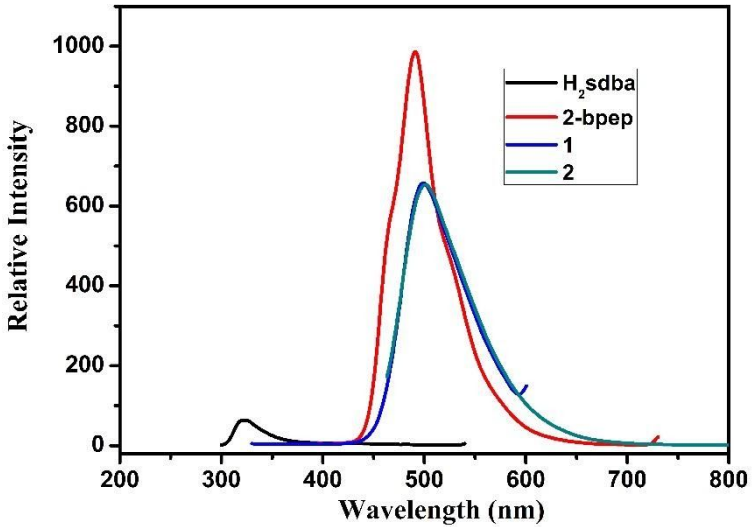

Fig. 4. The emission spectra of 2-bpeb, H_2sdba, **1** and **2**.

Detection of Anions

The striking fluorescence properties of **1** and **2** and their water-stability inspired us to investigate these complexes as potential fluorescent sensory materials in aqueous systems. Prior to the sensing experiments, the as-synthesized samples of **1** and **2** were fully ground and soaked in deionized water with ultrasonic treatment to obtain stable suspensions (1 mg/mL^{-1}). The different anion solutions (1 M, 100 μL and the corresponding cation is Na^+) were then added dropwise, which included F^-, Cl^-, Br^-, I^-, CO_3^{2-}, HCO_3^-, CH_3COO^- (AC^-), NO_3^-, SO_4^{2-}, SO_3^{2-}, $H_2PO_4^-$, HPO_4^{2-}, PO_4^{3-}, SiO_3^{2-}, ClO_4^-, BF_4^- and $Cr_2O_7^{2-}$, to the suspensions of **1** and **2**. The formula $(I_0\text{-}I)/I_0\times100\%$ was used to calculate the quenching efficiencies and the results are depicted in **Fig. 5**. It can be seen from the figure that different anions have different effects on the fluorescence intensity of **1** - **2**. Clearly, $Cr_2O_7^{2-}$ can almost quench the fluorescence emission of **1** - **2**, while other anions have almost no effect on the fluorescence emission.

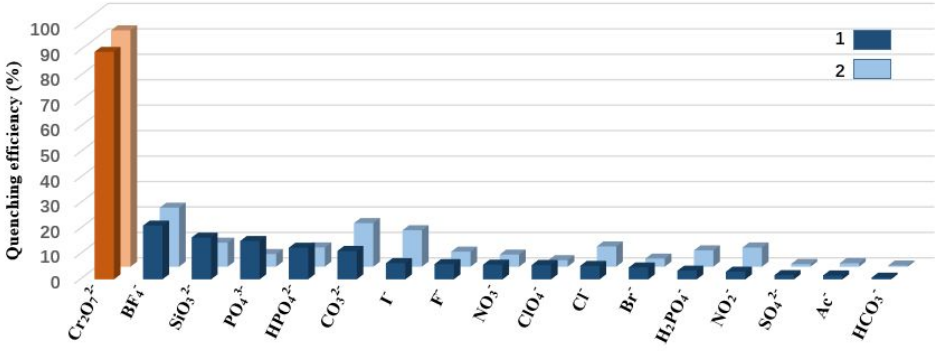

Fig. 5. The quenching efficiency of the suspensions of **1** - **2** upon addition of different anions.

To investigate the sensitivity of **1 - 2** towards $Cr_2O_7^{2-}$, quantitative fluorescence titration experiments have been conducted, which involved the gradual addition of an aqueous solution of $Cr_2O_7^{2-}$ (10 mM) to the suspension of **1-2**. **Fig. 6** shows the results of the fluorometric titrations of the two sensors with $Cr_2O_7^{2-}$. The complexes **1 - 2** were excited at 404 nm with an emission maximum at 495 nm, respectively. Upon addition of $Cr_2O_7^{2-}$, the sensors display a dramatic quenching of the fluorescence emission. The fluorescence quenching efficiencies and constants were analyzed by plotting the relative intensities against the concentration of $Cr_2O_7^{2-}$ and the plots are near linear over the low concentration range. The linear Stern-Volmer (SV) equation, $(I_0/I)=1+K_{SV}[A]$, was used to calculate the quenching constants, where I_0 and I are the emission intensities of the aqueous suspension before and after the addition of the aqueous solution of $Cr_2O_7^{2-}$; K_{SV} is the quenching constant, and [A] is the concentration of $Cr_2O_7^{2-}$. The results show that the correlation coefficients (R^2) of both linear regression equations are greater than 0.99.

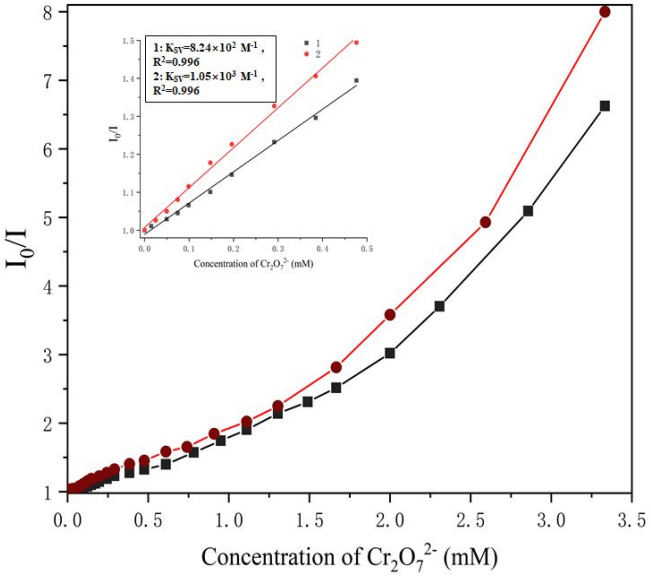

Fig. 6. The relative intensities of **1 - 2** on addition of $Cr_2O_7^{2-}$ (insert: Relative intensity was calculated by using the equal: $I/I_0\times100\%$.)

Detection of Cations

In addition to the identification of anions, we also conducted identification experiments on cations using **1 - 2**. As before, prior to the sensing experiments, the as-synthesized samples of **1** and **2** were fully ground and soaked in deionized water with ultrasonic treatment to obtain stable suspension (1 mg/mL^{-1}). The different cation solutions (1 M, 100 μL and the corresponding anion is Cl^-) were then added, including

Zn^{2+}, Co^{2+}, K^{+}, Cd^{2+}, Pb^{2+}, Al^{3+}, Cs^{+}, Mg^{2+}, Ca^{2+}, Rb^{+}, Na^{+}, Cr^{2+}, Ni^{2+}, Cu^{2+}, Mn^{2+}, Fe^{2+} and Fe^{3+}, dropwise to the suspension of **1** and **2**. The same method as above was used to obtain the data for **Fig. 7**. It is not difficult to find from the figure that different cations have different effects on the fluorescence intensity of **1** - **2**. Different from the anion recognition, a variety of cations quench the fluorescence emission of **1** - **2**, with Fe^{3+} producing the most dramatic quenching followed by Cr^{3+}.

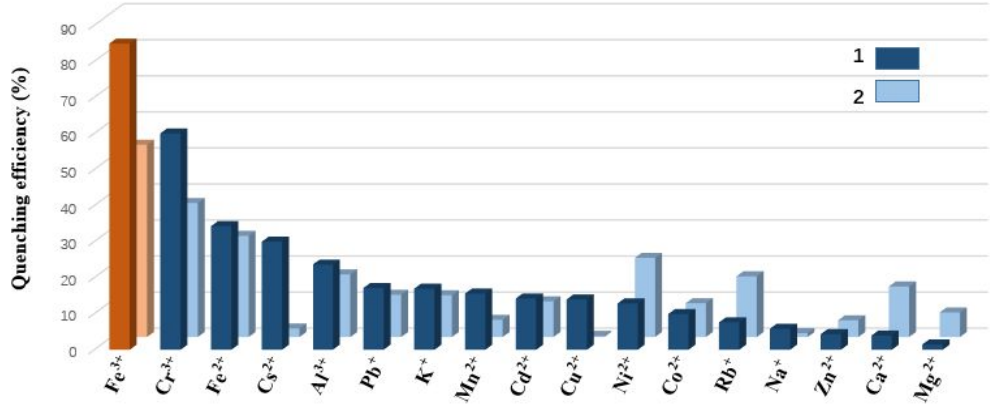

Fig. 6. The quenching efficiency of the suspension of **1** - **2** upon addition of different cations.

We have conducted quantitative fluorescence titration experiments involving the gradual addition of aqueous solution of Fe^{3+} (10 mM) to the suspensions of **1** - **2**. **Fig. 7** shows the results of the fluorometric titration of the two sensors with Fe^{3+}. The fluorescence quenching efficiencies and constants were analyzed by plotting the relative intensities against the concentration of Fe^{3+}. Unlike $Cr_2O_7^{2-}$, a linear relationship at both low and high concentrations is observed. By use of the linear Stern-Volmer (SV) equation to calculate the quenching constants, it is found that the correlation coefficients (R^2) of both linear regression equations are greater than 0.99.

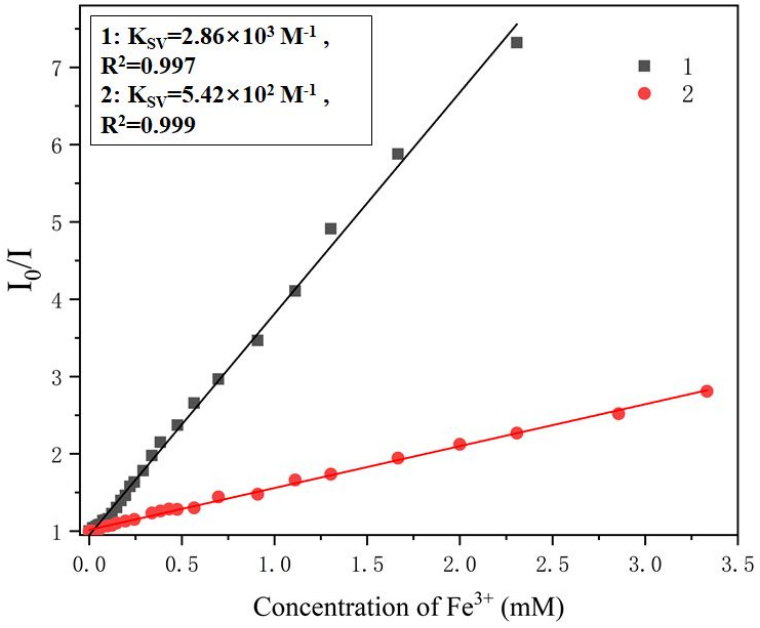

Fig. 7. The relative intensities of **1** - **2** with the addition of Fe^{3+} (insert: Relative intensity was calculated by using the equal: $I/I_0 \times 100\%$.)

Multiple use of a luminescent sensor increases its potential value for practical applications. Hence, the recycling performance of **1** - **2** as luminescent probes for the detection of iron and chromate ions was investigated. The dispersed Zn−MOF in the aqueous solution of Fe^{3+} and $Cr_2O_7^{2-}$ ions was recovered after the sensing experiment. The resulting solid was centrifuged multiple times with H_2O to wash off residual Fe^{3+} and $Cr_2O_7^{2-}$ ions from the surface. The PXRD pattern of the recovered samples after each cycle of sensing shows that the structure remains unaffected even after several cycles (**Fig. 2**). Clearly, **1** - **2** can be described as a stable, reusable, and versatile luminescent probes for sensing $Cr_2O_7^{2-}$ and Fe^{3+}ions in water.

According to previous literature,[27-35] the quenching effect on the fluorescence of MOFs by Fe^{3+} and $Cr_2O_7^{2-}$ could be ascribed to three aspects: (1) the collapse of the crystal structure; (2) the ion exchange in the framework with the targeted ions; (3) energy transfer between the ions and the CPs. The PXRD patterns of **1** and **2** reveal that their crystal structures remain intact and unchanged in the Fe^{3+} and $Cr_2O_7^{2-}$ ion solutions (Fig. 2), thus the structural collapse could be excluded. The frameworks of **1** and **2** are neutral; thus, capturing Fe^{3+} or $Cr_2O_7^{2-}$ via ions exchange is very difficult, which also could be confirmed by the ICP results. Moreover, the UV-vis absorption spectra of the Fe^{3+} and $Cr_2O_7^{2-}$ ions in aqueous solution were obtained. As shown in **Fig. S1**, the absorption bands of Fe^{3+} and $Cr_2O_7^{2-}$ both exhibit an extensive overlap with the emission bands of **1** and **2**, suggesting that the resonance energy transfer may

take place and lead to the fluorescence quenching.

Conclusions

In conclusion, two new isomorphic MOFs [Cd(2-bpeb)(a)] (**1**) and [Zn(2-bpeb)(sdba)] (**2**) were synthesized successfully by employing the mixed pro-ligand strategy by using 2-(4-((E)-2-(pyridine-2-yl)-vinyl)styryl)pyridine (2-bpeb) as the *N*-donor and H_2sdba as the *O*-donor under hydrothermal conditions. Single crystal X-ray diffraction reveals that both **1** and **2** are 3D frameworks with 1D channels constructed by 2D layers through non-convent interactions. Due to the existence of the large π-conjugated moieties and the d^{10} metal center, both **1** and **2** exhibit striking fluorescence properties and can function as chemical sensors via rapid luminescence quenching properties toward Fe^{3+} and $Cr_2O_7^{2-}$ in aqueous media with high sensitivity and selectivity.

Acknowledgements

We thank the National Natural Science Foundation of China Grant No. 21601090 and the Natural Science Foundation of Jiangsu Province (BK20160943), Jiangsu Province Graduate Training Practice Innovation Program (KYCX20_0961), and the Innovation and Entrepreneurship Training Program of Nanjing University of Information Science and Technology for financial support. CR thanks the EPSRC for an Overseas Travel Grant (EP/R023816/1).

Supplementary materials

CCDC NO. 2015015 - 2015016 contain the supplementary crystallographic data for this paper. The data can be obtained free of charge via www.ccdc.cam.ac.uk/data_request/cif (or from The Cambridge Crystallographic Data Centre, 12, Union Road, Cambridge CB2 1EZ, UK; fax: +44 1223 336 033; e-mail: deposit@ccdc.cam.ac.uk).

Conflicts of interest

There are no conflicts to declare.

References

[1] D. Burrows, Chromium – Metabolism and Toxicity, CRC Press, Boca Raton, FL, 1983.

[2] M. A. Tofighy, T. Mohammadi, J. Hazard Mater., 185 (2011) 140-147.

[3] M. Zheng, H. Q. Tan, Z. G. Xie, L. G. Zhang, X. B. Jing, Z. C. Sun, ACS Appl. Mater. Interfaces, 5 (2013) 1078-1083.

[4] B.-B. Lu, W. Jiang, J. Yang, Y.-Y. Liu, J.-F. Ma, ACS Appl. Mater. Interfaces, 45 (2017) 39441-39449.

[5] H. Li, M. Eddaoudi, M. O'Keeffe, O. M. Yaghi, Nature, 402(1999) 276-279.

[6] H. Li, K. Wang, Y. Sun, C. T. Lollar, J. Li, H.-C. Zhou, Mater. Today, 21(2018), 108-121.

[7] X. Zhao, Y. Wang, D. S. Li, X. Bu, P. Feng, Adv. Mater., 30 (2018) 1705189.

[8] Z. Zhang, Y. Zhao, Q. Gong, Z. Li, J. Li, Chem. Commun., 49 (2013) 653-661.

[9] D. Yang, B. C. Gates, ACS Catal., 9 (2019) 1779-1798.

[10] J. Qiu, X. Zhang, Y. Feng, X. Zhang, H. Wang, J. Yao, Appl. Catal. B, 231 (2018) 317-342.

[11] S. Vilela, T. Devic, A. Varez, F. Salles, P. Horcajada, Dalton Trans., 48 (2019) 11181-11185.

[12] B. L. Hou, D. Tian, J. Liu, L. Z. Dong, S. L. Li, D. S. Li, Y. Q. Lan, Inorg. Chem. 55 (2016) 10580-10586.

[13] Y. N. Gong, L. Jiang, T. B. Lu, Chem. Commun., 49 (2013) 11113-11115.

[14] W. Yan, C. L. Zhang, S. G. Chen, L. J. Han, H. G. Zheng, ACS Appl. Mater. Interfaces, 9 (2017) 1629-1634.

[15] Y. Wu, G.-P. Yang, Y. Zhao, W.-P. Wu, B. Liu, Y.-Y. Wang, Dalton Trans., 44 (2015) 10385-10391.

[16] S. Chen, Z. Shi, L. Qin, H. Jia, H. Zheng, Cryst. Growth Des., 17 (2017) 67-72.

[17] Y.-T. Yan, J. Liu, G.-P. Yang, F. Zhang, Y.-K. Fan, W.-Y. Zhang, Y.-Y. Wang, CrystEngComm., 20 (2018) 477-486.

[18] D. Zhao, X.-H. Liu, Y. Zhao, P. Wang, Yi Liu, M. Azam, S. I. Al-Resayes, Y. Lu, W.-Y. Sun, J. Mater. Chem. A, 5 (2017) 15797-15807.

[19] X.-D. Zhang, J.-A. Hua, J.-H. Guo, Y. Zhao, W.-Y. Sun, J. Mater. Chem. C, 6 (2018) 12623-12630.

[20] X.-D. Zhang, Y. Zhao, K. Chen, Y.-F. Jiang, W.-Y. Sun, Chem. Asian J., 13 (2019) 3620-3626.

[21] SAINT, *Program for Data Extraction and Reduction*, Bruker AXS, Inc.,

Madison, WI, 2001.

[22] G. M. Sheldrick, *SADABS*, *Program for Empirical Adsorption Correction of Area Detector Data*. University of Gottingen, Gottingen, Germany, 2003.

[23] (a) G. M. Sheldrick, *SHELXS-97, Program for the Crystal Structure Solution*, University of Gottingen, Gottingen, Germany, 1997; (b) G. M. Sheldrick, *SHELXL-97, Program for the Crystal Structure Solution*, University of Gottingen, Gottingen, Germany, 1997.

[24] L. Luo, K. Chen, Q. Liu, Y. Lu, T.-a. Okamura, G.-C. Lv, Y. Zhao, W.-Y. Sun, Cryst. Growth Des., 13 (2013) 2312−2321.

[25] M. D. Allendorf, C. A. Bauer, R. K. Bhakta, R. J. T. Houk, Chem Soc. Rev., 38 (2009) 1330.

[26] L. P. Zhang, J. F. Ma, J. Yang, Y. Y. Pang, J. C. Ma, Inorg. Chem., 49 (2010) 1535.

[27] B. Parmar, Y. Rachuri, K. K. Bisht, R. Laiya, E. Suresh, Inorg. Chem., 56 (2017) 2627.

[28] R. Lv, J. Y. Wang, Y. P. Zhang, H. Li, L. Y. Yang, S. Y. Liao, W. Gu, X. Liu, J. Mater. Chem. A., 4 (2016) 15494.

[29] M. Chen, W. M. Xu, J. Y. Tian, H. Cui, J. X. Zhang, C. S. Liu, M. Du, J. Mater. Chem. C., 5 (2017) 2015-2021.

[30] X. Y. Xu, B. Yan, ACS Appl. Mater. Interfaces, 7 (2015) 721.

[31] S. Pramanik, C. Zheng, X. Zhang, T. J. Emge, J. Li, J. Am. Chem. Soc., 133 (2011) 4153.

[32] Y. J. Yang, M. J. Wang, K. L. Zhang, J. Mater. Chem. C., 4 (2016) 11404.

[33] W. Q. Tong, T. T. Liu, G. P. Li, J. Y. Liang, L. Hou, Y. Y. Wang, New J. Chem., 42 (2018) 9221.

[34] B. Wang, Q. Yang, J. R. Li, ACS Appl. Mater. Interfaces, 9 (2017) 10286.

[35] B. Parmar, Y. Rachuri, K. K. Bisht, R. Laiya, E. Suresh, Inorg. Chem., 56 (2017) 2627.